

Effects of linear and nonlinear piezoelectricity on the electronic properties of InAs/GaAs quantum dots

Gabriel Bester,¹ Alex Zunger,¹ Xifan Wu,² and David Vanderbilt²

¹National Renewable Energy Laboratory, Golden, Colorado 80401, USA

²Department of Physics and Astronomy, Rutgers University, Piscataway, New Jersey 08854, USA

(Received 2 May 2006; published 22 August 2006)

The existence of enormous strain fields in self-assembled quantum dots has led to the expectation of dramatic effects of piezoelectricity. However, only linear piezoelectric tensors were used in all previous calculations. We calculate the piezoelectric properties of self-assembled quantum dots using the linear and quadratic piezoelectric tensors derived from first-principles density functional theory. We find that the previously ignored quadratic term has similar magnitude as the linear term and the two terms tend to cancel each other. We show the effect of piezoelectricity on electron and hole energy levels and wave functions as well as on correlated absorption spectra.

DOI: 10.1103/PhysRevB.74.081305

PACS number(s): 78.67.Hc, 73.21.La, 73.22.-f, 71.15.-m

The engineering of stain-induced self-assembled semiconductor quantum dots relies on a mismatch $\Delta a = a - a_0$ between the lattice constant of the dot material a and the lattice constant of the substrate a_0 on which the dots are grown.¹ The ensuing strain inside the quantum dots can be significantly larger than in ordinary (i.e., flat, parallel interfaces) semiconductor heterostructures because in the latter case large strains must be avoided to prevent dislocations ($\Delta a/a \leq 2\%$) whereas in nonflat geometries of InAs quantum dots grown on GaAs even $\Delta a/a \approx 7\%$ can be tolerated. In zincblende quantum well superlattices having parallel interfaces the piezoelectric field appears only if grown on specific substrate directions, strongest for [111], while it vanishes by symmetry for [100]. However, in three-dimensional lens-shaped quantum dots even the conventional [100] growth direction leads as a result of curvature to all types of strains (diagonal and off diagonal), which give rise to piezoelectric behavior. Indeed, large piezoelectric effects were suggested for [100]-grown quantum dots a decade ago.² Since then, a number of electronic structure calculations of quantum dots using $\mathbf{k} \cdot \mathbf{p}$ (Refs. 2–5) and atomistic methods⁶ have been performed taking the hitherto known *linear* piezoelectric effect into account and demonstrating important electronic consequences of piezoelectricity such as splitting of P levels, rotation of wave function lobes, and a strong decay of fine-structure splitting with increasing gaps.⁷ Recently,⁸ we calculated the piezoelectric tensors of GaAs and InAs from first principles and found surprisingly large nonlinear components.⁸ Applications to conventional quantum wells revealed a piezoelectric field with very strong contributions from the second-order piezoelectric terms that were previously neglected. In this paper we study the effect of nonlinearities of the piezoelectric effect on electronic and optical properties of quantum dots and find that the quadratic and linear piezoelectric effects tend to oppose each other. In fact, neglecting the piezoelectric effect is a better approximation than using only the linear term. We present a simple procedure for accurately incorporating both linear and nonlinear piezoelectric effects in all non-self-consistent calculations (e.g., effective mass, $\mathbf{k} \cdot \mathbf{p}$ or tight binding).

A self-consistent calculation of the electronic structure of

a deformed solid naturally includes the field generated by piezoelectric displacements. However, such a calculation requires the inclusion of all occupied energy levels and their response to strain and is thus limited to small systems. When considering large ($\geq 10^3$ atoms) nanostructures, it is often impractical to compute all occupied levels, and one prefers to concentrate on only a few (≈ 100) states in the physical range of interest. By necessity, in such cases (effective mass, $\mathbf{k} \cdot \mathbf{p}$, or any few-band calculation) the calculation is no longer self-consistent, and piezoelectricity does not arise naturally, but has to be added as an external potential V_{piezo} . In the pseudopotential representation the total potential used for the single-particle Schrödinger equation is $V_{\text{tot}}(\mathbf{r}) = V_{\text{PS}}(\mathbf{r}) + V_{\text{piezo}}(\mathbf{r})$ where V_{PS} is the superposition of $\sim 2 \times 10^6$ screened atomic potentials, including spin-orbit interaction.

The calculation of the piezoelectric potential V_{piezo} is performed in four steps. In the first step we calculate the linear and nonlinear piezoelectric coefficients \tilde{e} and \tilde{B} of strained *bulk* GaAs and InAs (Ref. 9) using linear response density functional theory. This was done in Ref. 8. In the second step, the polarization is calculated to second order in strain as

$$p_\mu = \sum_j \tilde{e}_{\mu j}^0 \eta_j + \frac{1}{2} \sum_{jk} \tilde{B}_{\mu jk} \eta_j \eta_k, \quad (1)$$

where η is the strain in Voigt notation, and \tilde{e} and \tilde{B} are the piezoelectric tensors. In the third step, the piezoelectric density is calculated from the divergence of the polarization:

$$\rho_{\text{piezo}}(\mathbf{r}) = -\frac{e}{a_0} \nabla \cdot \mathbf{p}; \quad (2)$$

and in the final step, the potential $V_{\text{piezo}}(\mathbf{r})$ is obtained from the solution of the Poisson equation:

$$\rho_{\text{piezo}}(\mathbf{r}) = \epsilon_0 \nabla \cdot [\epsilon_s(\mathbf{r}) \nabla V_{\text{piezo}}(\mathbf{r})]. \quad (3)$$

More details of the calculations are given in Ref. 8.

With the piezoelectric potential added to V_{PS} , the ensuing Schrödinger equation is solved within a basis constructed from a linear combination of strained bulk bands (LCBB

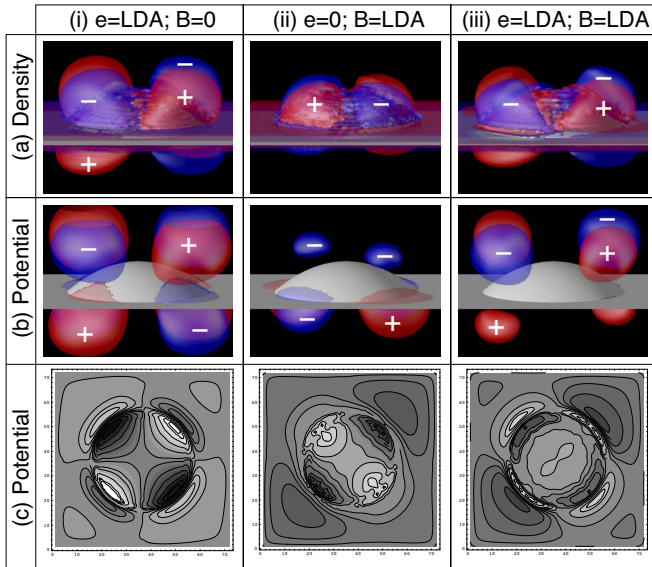


FIG. 1. (Color online) (a) Piezoelectric density of an InAs quantum dot with 25 nm base and 5 nm height. The isosurfaces represent $\pm 0.003e/\text{a.u.}^3$. (b) Corresponding piezoelectric potential with isosurfaces at ± 35 mV. (c) Contour plots of the piezoelectric potential 1 nm above the wetting layer. The maximum value of the potential is 28 mV and the minimum is 29 mV. The three columns correspond to (i) neglect of $\tilde{B}_{\mu jk}$, (ii) neglect of $\tilde{e}_{\mu j}$, and (iii) retention of both $\tilde{e}_{\mu j}$ and $\tilde{B}_{\mu jk}$.

method¹⁰). The many-body properties are obtained from a configuration-interaction treatment¹¹ based on such single-particle states. This approach (but without V_{piezo}) has been used successfully in many occasions in the past.^{12,13}

Figure 1 shows the piezoelectric density [Eq. (2)] and the piezoelectric potential [Eq. (3)]. The gray surface visible in Fig. 1(b) shows the physical shape of the quantum dot: a lens-shaped quantum dot with 25 nm base diameter and 5 nm height. The contour plots in Fig. 1(c) represent (001) planes located 1 nm above the base of the dot. The density

and potential are shown for three scenarios regarding the piezoelectric coefficients: (i) $\tilde{e}_{\mu j}$ at the local density approximation (LDA) value, $\tilde{B}_{\mu jk}=0$, i.e., where the linear term is set to the value obtained from the *ab initio* calculations and the nonlinear term $\tilde{B}_{\mu jk}$ is set to zero; (ii) $\tilde{e}_{\mu j}=0$, $\tilde{B}_{\mu jk}$ at the LDA value, and (iii) both $\tilde{e}_{\mu j}$ and $\tilde{B}_{\mu jk}$ at the LDA values. Remarkably we see that the linear and quadratic terms tend to compensate each other in the piezoelectric density and potential. While the linear term gives rise to *negative* density regions along the [110] direction, the quadratic term shows *positive* densities along this direction. A similar compensating behavior can be observed for the potential. Indeed, the linear term attracts the electrons to the $[1\bar{1}0]$ direction while the second-order term attracts them to the [110] direction. The opposite is true for holes. The compensation is not perfect, and the resulting total potential [column (iii) in Fig. 1] exhibits a complex residual behavior. The potential is fairly isotropic around the center of the dot, with a convoluted landscape of positive and negative potentials around the periphery of the dot. Thus a visual inspection of the potential does not disclose the response of electrons and holes to piezoelectricity. We will next discuss the importance and qualitative effects of piezoelectricity.

Figure 2 shows the single-particle eigenvalues of the electron and hole states in lens shaped InAs/GaAs quantum dots with different heights [Figs. 2(b) and 2(d)] and base diameters [Figs. 2(a) and 2(c)]. We compare the results obtained with full (solid lines) and without (dashed lines) piezoelectric effect. On the scale of the electron splitting energies between *S*, *P*, and *D* levels, the shifts of eigenvalues due to the piezoelectric effect are small, in the range of 0–8 meV. This is considerably smaller than the results obtained by retaining \tilde{e}_{14} alone. The effect seems stronger for the holes because of the smaller natural hole-level separation. The effect is stronger for tall dots.

To assess quantitatively the relative importance of the first- and second-order piezoelectric tensors we choose to focus on the energy splitting between the much discussed

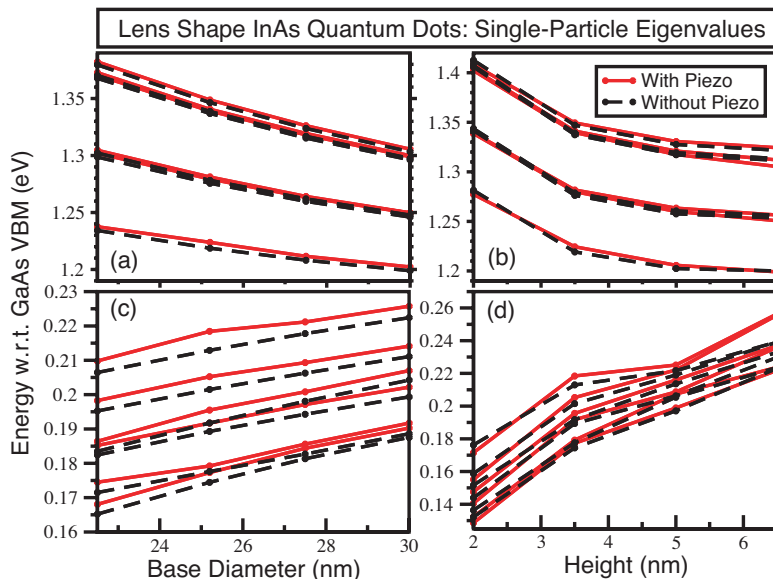


FIG. 2. (Color online) Single-particle eigenvalues, with respect to the GaAs valence band edge, of the electron [(a),(b)] and hole states [(c),(d)] in lens-shaped InAs/GaAs quantum dots with different heights [(b),(d)] keeping the base diameter at 25 nm and different base diameters [(a),(c)] keeping the height at 3.5 nm. Solid lines are results with piezoelectric effect and dashed lines without.

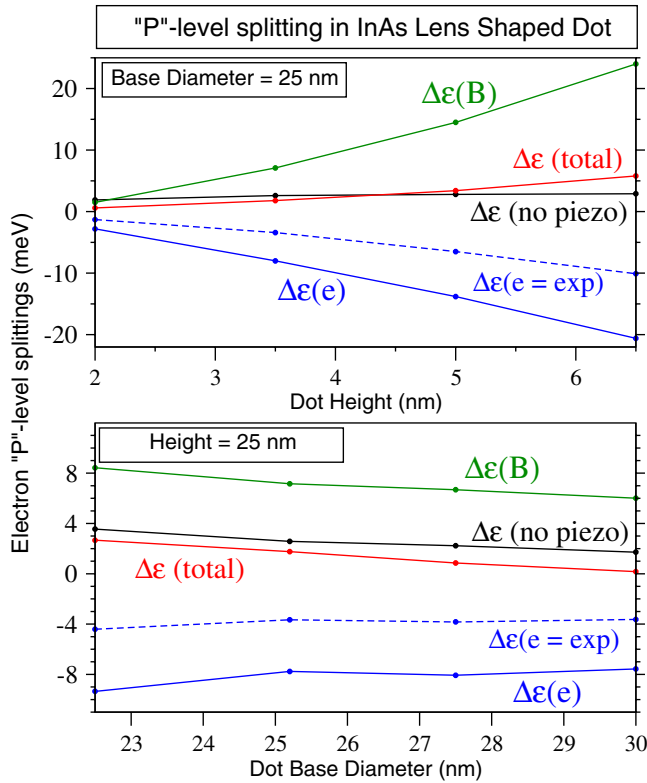


FIG. 3. (Color online) Splitting of the electron P states for a lens-shaped InAs/GaAs quantum dot decomposed into the (i) atomistic, (ii) linear piezoelectric, and (iii) quadratic piezoelectric contributions. The upper panel shows the height dependence of the splitting for a dot with 25 nm base diameter and the lower panel shows the base dependence for a dot with 3.5 nm height. The dashed lines give the contributions of the linear term when the experimental values of $\tilde{\epsilon}_{\mu j}$ are used.

electron P states (second and third electron states) $\Delta\epsilon = \epsilon(P_{[110]} - P_{[\bar{1}\bar{1}0]})$. $\Delta\epsilon$ has three different sources: (i) an atomistic contribution [$\Delta\epsilon$ (no piezo)] that exists even without V_{piezo} and originates from the (atomistic) C_{2v} symmetry of the quantum dot (see Ref. 6 for a discussion of this effect); (ii) the contribution [$\Delta\epsilon(e)$] from the linear piezoelectric term, obtained by setting the quadratic term $\tilde{B}_{\mu j k}$ to zero in Eq. (1) and subtracting the atomistic splitting; (iii) the contribution [$\Delta\epsilon(B)$] from the quadratic piezoelectric term, obtained by setting the linear term $\tilde{\epsilon}_{\mu j}$ to zero in Eq. (1) and subtracting the atomistic splitting. In Fig. 3 we plot the base and height dependence of $\Delta\epsilon$ for lens-shaped InAs/GaAs quantum dots. We see that the effects of the linear and the quadratic terms have opposite signs and have very similar magnitude. This cancellation of the effect is observed for all dot heights and base sizes considered here. The final result for the splitting is then very close to the atomistic splitting obtained without V_{piezo} and is generally small (from 0 to 6 meV) and positive, showing also that the first electron P state is oriented along the $[\bar{1}\bar{1}0]$ direction. The results [$\Delta\epsilon(e=\text{exp})$] for the linear contribution using the experimental values of $\tilde{\epsilon}_{\mu j}$, is given as a dashed line. It represents the approximation that has been used in the literature so far²⁻⁵ and shows that it leads to qualitative errors with the wrong

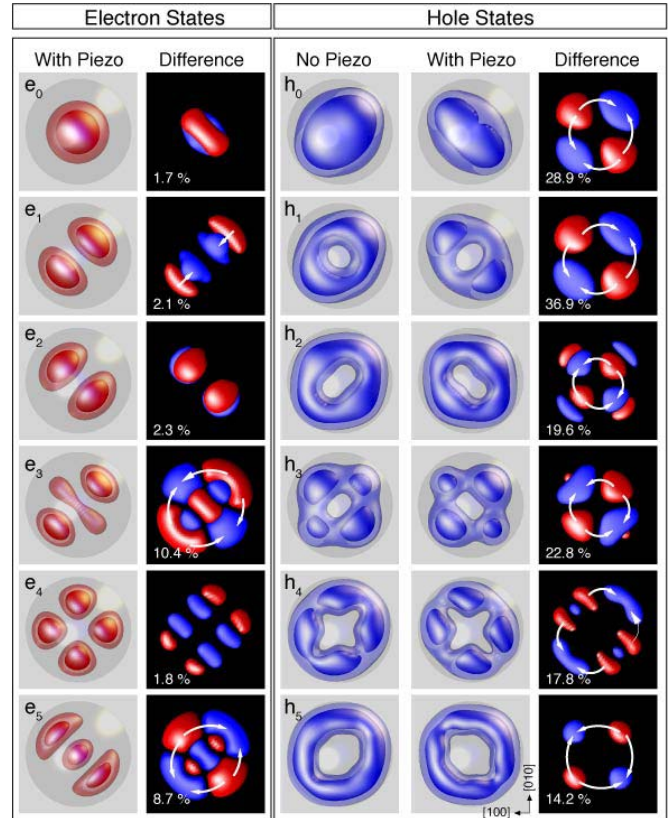


FIG. 4. (Color online) Square of the electron (left) and hole (right) single-particle wave functions for an InAs/GaAs lens-shaped quantum dot with 25 nm base and 5 nm height. The inner (outer) isosurface encloses 45% (75%) of the state density. The second and fifth columns show the charge transfer upon inclusion of piezoelectricity and the numbers give the percentages of one electron charge transferred.

sign for the splitting and a magnitude too large by a factor of up to 5. It is in fact more accurate to neglect the piezoelectric effect altogether than use the linear coefficients alone.

Figure 4 shows a top view of isosurfaces of the square of the single-particle wave functions ψ for the first six confined states, looking down along the $[00\bar{1}]$ direction. All plots are for a lens-shaped InAs/GaAs quantum dot with 25 nm base and 5 nm height. The columns with the black backgrounds show the difference $|\psi_{\text{piezo}}(\mathbf{r})|^2 - |\psi(\mathbf{r})|^2$ and the arrows indicate where charge is flowing when full piezoelectricity is included. The *electron* wave functions do not change qualitatively when piezoelectricity is taken into account. The amount of charge that is redistributed due to the piezoelectric effect ranges from 1.7% to 10.4%, in units of one electron charge. For the states e_0 , e_1 , and e_2 the charge is mainly redistributed in the $[001]$ direction with an increase of charge toward the top of the dot for e_0 and e_2 and toward the bottom for e_1 . The D states e_3 , e_4 , and e_5 have some charge redistribution in plane which is most significant for e_3 and e_5 . The complexity of the piezoelectric potential landscape becomes more apparent from this picture. There is no obvious preferred direction along which the states will extend, e.g., state e_3 seems to become more extended along the $[110]$ direction while state e_5 extends along $[\bar{1}\bar{1}0]$. This is in agreement with

the P -level splitting results from Fig. 2. Since linear and quadratic effects are of very similar magnitude, the overall effect becomes more subtle.

The results for the *hole* wave functions show a larger redistribution of charge between 14.2% to 36.9% of an electron charge. The redistribution is exclusively in the (001) plane, with no change along [001]. For tall dots with $h \geq 5$ nm the piezoelectric effect changes qualitatively the symmetry of the hole wave function, altering the dominant orientation of the states h_0 and h_1 . For the conventionally grown flatter dot with 3.5 nm height there is no qualitative change (e.g., rotation of the wave functions). The charge redistribution is between 5.2% and 8.9%.

The symmetry of the wave function is indirectly reflected by the intensities and the polarization of optical transitions. In Fig. 5 we show the absorption spectrum, calculated via configuration interaction, of the lens-shaped quantum dot with 25 nm base and 5 nm height with and without the inclusion of the piezoelectric effect. We see some changes in the energy splitting of the P - P transitions as expected from the single-particle results of Fig. 2, and some changes in the relative oscillator strength of these transitions. The polarization anisotropy is calculated as $\lambda = [I_{[110]} - I_{[1\bar{1}0]}] / [I_{[110]} + I_{[1\bar{1}0]}]$ where I is the intensity. The S - S transition is 5% polarized without piezo and 9% with piezo. The four main P - P transitions have 9%, 5%, 18%, 18% polarization without piezo and 3%, 23%, 27%, 33% when piezoelectricity is included.

The fine structure is the splitting between the bright exciton states due to electron-hole exchange interaction and is normally $\leq 100 \mu\text{eV}$ and has been accounted for experimentally¹⁴ and theoretically.¹⁵ However, recently, Seguin *et al.*⁷ reported giant fine-structure splittings of 500 μeV in dots of unspecified structure. The origin of the splitting was suggested to be piezoelectricity on the grounds

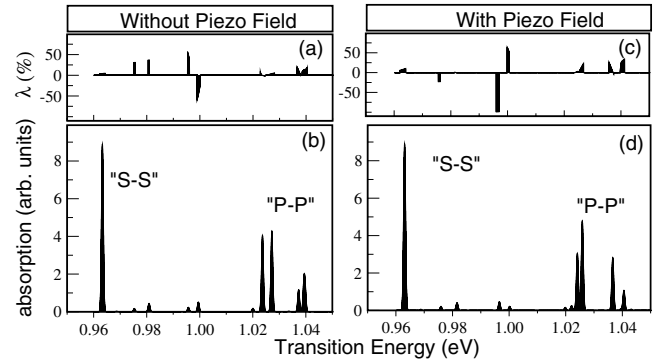


FIG. 5. Optical absorption [(b),(d)] and anisotropy λ [(a),(c)] of a lens-shaped quantum dot with $b=25$ nm and $h=5$ nm, with [(c),(d)] and without [(a),(b)] piezoelectric effect.

of calculations done using a very large value of $\tilde{\epsilon}_{14}$ (eight times larger than the experimental value) and neglecting the quadratic $\tilde{B}_{\mu jk}$ terms. Our own fine-structure results using linear and quadratic terms show almost no influence of the piezoelectric field on the fine-structure splittings. The reason for the very large measured splittings in Ref. 7 remains therefore unexplained.

In summary, we have shown that the quadratic piezoelectric terms must be taken into account for quantitative calculations of the effect of piezoelectricity on the electronic and optical properties of quantum dots. If the quadratic tensors are unknown, it is better to neglect piezoelectricity altogether than to simply include the linear term.

This work has been supported by U.S. DOE Grant No. SC-BES-DMS under the LAB-03-17 initiative and by NSF Grant No. DMR-0233925.

¹V. Shchukin and D. Bimberg, Rev. Mod. Phys. **71**, 1125 (1999).

²M. Grundmann, O. Stier, and D. Bimberg, Phys. Rev. B **52**, 11969 (1995).

³O. Stier, M. Grundmann, and D. Bimberg, Phys. Rev. B **59**, 5688 (1999).

⁴M. A. Migliorato, D. Powell, S. L. Liew, A. G. Cullis, P. Navarette, M. J. Steer, M. Hopkinson, M. Fearn, and J. H. Jefferson, J. Appl. Phys. **96**, 5169 (2004).

⁵C. Pryor, Phys. Rev. B **57**, 7190 (1998).

⁶G. Bester and A. Zunger, Phys. Rev. B **71**, 045318 (2005).

⁷R. Seguin, A. Schliwa, S. Rodt, K. Potschke, U. W. Pohl, and D. Bimberg, Phys. Rev. Lett. **95**, 257402 (2005).

⁸G. Bester, X. Wu, D. Vanderbilt, and A. Zunger, Phys. Rev. Lett. **96**, 187602 (2006).

⁹For InAs we use (in C/m^2) $\tilde{\epsilon}_{14} = -0.115$; $\tilde{B}_{114} = -0.531$; $\tilde{B}_{124} = -4.076$; $\tilde{B}_{156} = -0.120$ and for GaAs $\tilde{\epsilon}_{14} = -0.230$; $\tilde{B}_{114} = -0.439$; $\tilde{B}_{124} = -3.765$; $\tilde{B}_{156} = -0.492$. From the three independent tensor

components \tilde{B}_{114} , \tilde{B}_{124} , and \tilde{B}_{156} the other 21 nonzero elements can be obtained by applying cyclic permutations $x \rightarrow y \rightarrow z$, interchanges such as $x \leftrightarrow y$, and exchange of the two Voigt indices.

Thus, e.g., $\tilde{B}_{114} = \tilde{B}_{225}$, $\tilde{B}_{124} = \tilde{B}_{235} = \tilde{B}_{215}$, and $\tilde{B}_{156} = \tilde{B}_{264}$.

¹⁰L.-W. Wang and A. Zunger, Phys. Rev. B **59**, 15806 (1999).

¹¹A. Franceschetti, H. Fu, L.-W. Wang, and A. Zunger, Phys. Rev. B **60**, 1819 (1999).

¹²G. Bester, J. Shumway, and A. Zunger, Phys. Rev. Lett. **93**, 047401 (2004).

¹³L. He, G. Bester, and A. Zunger, Phys. Rev. Lett. **94**, 016801 (2005).

¹⁴M. Bayer, G. Ortner, O. Stern, A. Kuther, A. A. Gorbunov, A. Forchel, P. Hawrylak, S. Fafard, K. Hinzer K, T. L. Reinecke, S. N. Walck, J. P. Reithmaier, F. Klopff, and F. Schafer, Phys. Rev. B **65**, 195315 (2002).

¹⁵G. Bester, S. Nair, and A. Zunger, Phys. Rev. B **67**, 161306(R) (2003).